Wind and Structures, *Vol. 31, No. 1 (2020) 75-84*
DOI: https://doi.org/10.12989/was.2020.31.1.75

Nonlinear aerostatic analysis of long-span suspension bridge by Element free Galerkin method

Golriz Zamiri[a] and Saeed-Reza Sabbagh-Yazdi*

Department of Civil Engineering, KNToosi University of Technology, 1346, Valiasr St. (Mirdamad Cross), Tehran, Iran

(*Received September 14, 2018, Revised May 1, 2019, Accepted May 30, 2019*)

Abstract. The aerostatic stability analysis of a long-span suspension bridge by the Element-free Galerkin (EFG) method is presented in this paper. Nonlinear effects due to wind structure interactions should be taken into account in determining the aerostatic behavior of long-span suspension bridges. The EFG method is applied to investigate torsional divergence of suspension bridges, based on both the three components of wind loads and nonlinearities of structural geometric. Since EFG methods, which are based on moving least-square (MLS) interpolation, require only nodal data, the description of the geometry of bridge structure and boundaries consist of defining a set of nodes. A numerical example involving the three-dimensional EFG model of a suspension bridge with a span length of 888m is presented to illustrate the performance and potential of this method. The results indicate that presented method can effectively be applied for modeling suspension bridge structure and the computed results obtained using present modeling strategy for nonlinear suspension bridge structure under wind flow are encouragingly acceptable.

Keywords: suspension bridge; Element-free Galerkin methods; aerostatic stability; wind loads; wind structure interaction

1. Introduction

In the last decade, suspension bridges have been increasingly considered and now are one of the most significant kinds of long-span bridges. Owing to their high flexibility, the stability of suspension bridge due to wind loads is a significant subject in the design and construction of long-span suspension bridges.

The subject of aeroelastic behavior of suspension bridge has been studied for many years, and several numerical models (Selvam, Govindaswamy *et al*. 2002), (Zhang 2008), (Arena, Lacarbonara *et al*. 2014), (Arena, Lacarbonara *et al*. 2016) and experimental procedures have been proposed. Some experimental approaches are usually utilized to describe the bridge behavior to different static and dynamic wind loads (Diana, Fiammenghi *et al*. 2013), (Diana, Rocchi *et al*. 2015), (Ge, Xia *et al*. 2018). Hirai *et al*. (1967) and Cheng (2000) discovered that torsional divergence of the suspension bridges with long spans becomes apparent due to the action of static wind loads in wind tunnel tests of the bridge model. However, the experimental approaches could be costly, time consuming and somehow difficult to provide suitable real world conditions. Hence, developing numerical simulations of the bridge behavior is highly desirable for reducing the modeling time and increasing the accuracy and reliability of the computational results.

*Corresponding author, Professor
E-mail: syazdi@kntu.ac.ir
[a]Ph.D. Student
E-mail: golriz_Zamiri@yahoo.com

As a consequence of the fast growing computational power and the challenging issues of the scaled physical modeling, numerical method is being developed to protect or to replace the costly and time-consuming part of the experimental methods. Over the last recent years, the numerical study on the suspension bridge has been extensively performed by finite element method (FEM). For example, Arzoumanidis *et al*. (1985) explored the effects of steady and unsteady wind forces by using FEM. They developed a three-dimensional bridge structure model taking into consideration both the nonlinear material properties and the geometric nonlinearities of structural members (included cables and elements of deck system). They reported that the modeling of the external loads and the structural system of the bridge is realistically possible by the finite element method. Zhang *et al*. (2002) developed an approach of nonlinear aerostatic and aerodynamic analysis for long-span suspension bridges. Their reported results of numerical analysis for the three-dimensional finite element model demonstrated that the nonlinear effects significantly influence the aerostatic and aerodynamic behaviors of long-span suspension bridges. Petrini *et al*. (2007) applied four types of time domain techniques (including nonaeroelastic, steady, quasi steady, modified quasi steady) to investigate the response and the stability of a long-span suspension bridge. They considered a three dimensional finite element model of the bridge for analysis.

The aerostatic behavior of suspension bridges has been investigated by some studies. For example, Cheng *et al*. (2002), (2003) investigated nonlinear aerostatic stability analysis of the suspension bridge. They proposed a new nonlinear method to evaluate aerostatic stability of suspension bridges, based on the simultaneous effect of the geometric nonlinearity and the three components of wind

http://www.techno-press.com/journals/was&subpage=7 ISSN: 1226-6116 (Print), 1598-6225 (Online)

loads. A computer program NASAB were developed for their analysis. The results of these researches indicated that critical wind velocity of aerostatic instability considerably reduce as the effects of the geometric nonlinearity and the three-component displacement-dependent wind loads are simultaneously considered in the analysis. Other researchers like Boonyapinyo *et al*. (2006) performed nonlinear aerostatic stability analysis of long-span suspension bridges formulating wind induced aerostatic instability using the FEM. They considered material nonlinearity as well as three components of wind loads and geometric nonlinearity. The numerical modeling indicated that incorporation of geometric nonlinearity, material nonlinearity and nonlinear three-component displacement-dependent wind loads cause to occur the aerostatic instability in the long-span suspension bridge. In addition, they showed that the critical wind velocity for nonlinear aerostatic instability is appreciably less than the critical velocity of flutter instability. Zhang (2011) and Zhang *et al*. (2013) also evaluated the nonlinear aerostatic stability in long-span suspension bridges by FEM. The coupled influence of aerostatic loads and structural deformation was considered in these researches.

Hence, in addition to examining the elastic flutter analysis, it is necessary to perform accurate analysis of the nonlinear aerostatic instability of the bridge structure. Despite previous researches in this field, many problems in accurate numerical modeling still remain. The FEM is a robust and entirely developed method, and hence it is widely used in suspension bridge modeling due to its versatility for complex geometry and availability well developed commercially FEM packages (Duan, Xu *et al*. 2011), (Hong, Ubertini *et al*. 2011), (Kilic, Raatschen *et al*. 2017). However, the FEM has the inherent deficiency of numerical methods that rely on meshes or elements. Generally in using any FEM codes and packages, the creation of a mesh for a problem domain is required as a prior knowledge. Furthermore, resolving large movement and deformation of structures (which associate with aero-elastic behavior of cables and deck of the long-span suspended bridges) is still a challenging task for mesh based FEM analysis.

Usually a time consuming quality mesh generation for suspension bridge in three-dimensional domains becomes the major component of the modeling procedure. In addition to, under large deformations, considerable loss in accuracy in FEM results can arise from the element distortions. These issues can considerably affect the results obtained by FEM for aero-elastic analysis of a long-span suspension bridge. It can be stated that the root of these problems is the use of elements or mesh in the FEM. As an alternative solution of problem, the meshfree methods are developed with idea of getting rid of the elements and meshes in the process of numerical simulation.

The main objective of this study is to develop a nonlinear Element-free Galerkin (EFG) method to prevail drawbacks of mesh based methods to investigate the nonlinear aerostatic stability of suspension bridge. The nonlinear aerostatic stability analysis is presented by considering the simultaneous influences of nonlinearities of structural geometric and nonlinear three components displacement-dependent wind loads. The EFG method is utilized to evaluate the torsional divergence of a long-span suspension bridge with a main span of 888 meters assuming wind loads to be the function of the torsional response of structure. The numerical simulation is performed by programming in the MATLAB software framework.

2. Numerical implementation

The static response of problem with large deformation is considered in a domain Ω, bounded by Γ. The strong-form of system equation is given as follow

$$\boldsymbol{L}^{T}\boldsymbol{\sigma}+\boldsymbol{b}=0 \tag{1}$$

where is differential operator, is stress, is a body force vector (Liu and Gu 2010).

The common boundary conditions of above equation are as follows

$$\boldsymbol{\sigma n}=\bar{\boldsymbol{t}} \quad \text{in } \Gamma_t \tag{2}$$

$$u=\bar{u} \quad \text{in } \Gamma_u \tag{3}$$

where is displacement, is the vector of unit outward normal at a point on the natural boundary and and denote the prescribed displacements and tractions values, respectively (Liu and Gu 2010).

The constrained Galerkin weak-form should be posed as follows

$$\int_{\Omega}\delta(\boldsymbol{Lu})^{T}(\boldsymbol{\sigma})d\Omega-\int_{\Omega}\delta\boldsymbol{u}^{T}\boldsymbol{b}d\Omega-\int_{\Gamma_t}\delta\boldsymbol{u}^{T}\bar{\boldsymbol{t}}d\Gamma-\delta\int_{\Gamma_u}\frac{1}{2}(\boldsymbol{u}-\bar{\boldsymbol{u}})^{T}\boldsymbol{\alpha}(\boldsymbol{u}-\bar{\boldsymbol{u}})d\Gamma=0 \tag{4}$$

where is a diagonal matrix of penalty factors. In this paper, in order to impose essential boundary condition, the penalty method is used (Liu and Gu 2010).

3. Discrete equations

The main structural components of a suspended bridge include the deck, cables, hangers and towers. For the cable, hangers and deck, nonlinear geometrical effects are significant. Hence, in the present paper, the cable, hangers and deck are considered for numerical simulation of suspension bridge (Fig. 1). The geometric nonlinearities originate from the cable sag, the action of the loads due to the cables on the bridge deck that causes large deformations and the effect of the structure's relatively large deflection due to stresses and forces.

The EFG method, which is based on the Moving Least Squares approximation (MLS), requires only nodal data and no element connectivity, and thus has more flexibility than the conventional FEM.

Consider an unknown scalar function of a field variable

$u(x)$ in the domain Ω. The MLS approximation of $u(x)$ is described at an arbitrary point x as

$$u^h(x) = \sum_{j=1}^{m} p_j(x) a_j(x) = \boldsymbol{p}^T(\boldsymbol{x})\boldsymbol{a}(\boldsymbol{x}) \tag{5}$$

where presents the approximated function, is the basis function in the spatial coordinates and is the order of basis function (Liu and Gu 2010).

$$P^T(x) = \{1\ x\ x^2\ \ldots\ x^{m-1}\ x^m\} \tag{6}$$

and $\boldsymbol{a}(\boldsymbol{x})$ is a vector of coefficients given by

$$\boldsymbol{a}^T(\boldsymbol{x}) = \{a_1(\boldsymbol{x})\ \ a_2(\boldsymbol{x}) \ldots\ \ a_m(\boldsymbol{x})\} \tag{7}$$

The vector of coefficient $\boldsymbol{a}^T(\boldsymbol{x})$ is a function of $\boldsymbol{x}$.

The coefficients $\boldsymbol{a}(\boldsymbol{x})$ can be obtained by minimizing the following equation (Lancaster and Salkauskas 1981):

$$J = \sum_{i=1}^{n} \hat{W}(x - x_i)\left[\boldsymbol{p}^T(\boldsymbol{x}_i)\boldsymbol{a}(\boldsymbol{x}) - u_i\right]^2 \tag{8}$$

In the above, $\hat{W}(x - x_i)$ is a positive weighting function, n is the number of nodes in the support domain 犯and u_i refers to the nodal parameter of u at $\boldsymbol{x} = \boldsymbol{x}_i$.

The minimum of J with respect to $\boldsymbol{a}(\boldsymbol{x})$ leads to the following set of linear relations:

$$\boldsymbol{A}(\boldsymbol{x})\boldsymbol{a}(\boldsymbol{x}) = \boldsymbol{B}(\boldsymbol{x})\boldsymbol{u} \tag{9}$$

or

$$\boldsymbol{a}(\boldsymbol{x}) = \boldsymbol{A}^{-1}(\boldsymbol{x})\boldsymbol{B}(\boldsymbol{x})\boldsymbol{u} \tag{10}$$

where

$$\boldsymbol{A}(\boldsymbol{x}) = \sum_{i=1}^{n} \hat{W}_i(x - x_i)\boldsymbol{p}(\boldsymbol{x}_i)\boldsymbol{p}^T(\boldsymbol{x}_i) \tag{11}$$

and

$$\boldsymbol{B}(\boldsymbol{x}) = \left[\hat{W}_1(\boldsymbol{x})\boldsymbol{p}(\boldsymbol{x}_1), \hat{W}_2(\boldsymbol{x})\boldsymbol{p}(\boldsymbol{x}_2), \ldots, \hat{W}_n(\boldsymbol{x})\boldsymbol{p}(\boldsymbol{x}_n)\right] \tag{12}$$

$$\boldsymbol{u} = \{u_1\ u_2 \ldots\ u_n\}^T \tag{13}$$

By substituting (10) to (5), MLS approximation can be obtained as

$$u^h = \sum_{I}^{n} \Phi_I(\boldsymbol{x}) u_I = \boldsymbol{\Phi}^T(\boldsymbol{x})\boldsymbol{u} \tag{14}$$

where u^h presents the approximated displacements of a point which can be a quadrature point or a sampling point, the vector $\boldsymbol{u}$ collects the nodal parameters of u for all the nodes in the support domain and $\boldsymbol{\Phi}(\boldsymbol{x})$ is the vector of MLS shape functions corresponding n nodes in the support domain of the point $\boldsymbol{x}$.

The shape function $\Phi_I(\boldsymbol{x})$ for the Ith node is defined by

$$\begin{aligned}\Phi_I(\boldsymbol{x}) &= \sum_{j=1}^{m} p_j(\boldsymbol{x})\left(\boldsymbol{A}^{-1}(\boldsymbol{x})\boldsymbol{B}(\boldsymbol{x})\right)_{jI} \\ &= \mathbf{p}^T(\boldsymbol{x})\left(\boldsymbol{A}^{-1}\boldsymbol{B}\right)_I\end{aligned} \tag{15}$$

In this paper, the cubic spline weight function is used (Liu and Gu 2010)

$$\hat{W}_i(x - x_i) = \begin{cases} \dfrac{2}{3} - 4\bar{r}_i^2 + 4\bar{r}_i^3 & \bar{r}_i \le 0.5 \\ \dfrac{4}{3} - 4\bar{r}_i + 4\bar{r}_i^2 - \dfrac{4}{3}\bar{r}_i^3 & 0.5 < \bar{r}_i \le 1 \\ 0 & \bar{r}_i > 1 \end{cases} \tag{16}$$

where $\bar{r}_i = \dfrac{d_i}{r_w} = \dfrac{|x - x_i|}{r_w}$ in which $d_i = |x - x_i|$ presents the distance from node x_i to the sampling point x and r_w is the size of the support domain for the weight function (Liu and Gu 2010).

The MLS shape functions produced by n nodes in the local support domain are applied to approximate the displacement for major members of bridge, as follow:

- Deck

The bridge deck is adopted as a continuous beam.

$$\begin{aligned}\boldsymbol{u}^h &= \begin{Bmatrix} u \\ v \\ w \\ \Psi \end{Bmatrix} = \left[\phi_1\ \ \ldots\ \ \phi_n\right] \\ &\left[u_1, v_1, w_1, \theta_{x1}, \theta_{y1}, \theta_{z1}, \ldots, u_n, v_n, w_n, \theta_{xn}, \theta_{yn}, \theta_{zn}\right]^T \\ &= \boldsymbol{\Phi}_{4\times 6n}\boldsymbol{u}_{6n\times 1}\end{aligned} \tag{17}$$

- Suspended cable and Hangers

$$\begin{aligned}\boldsymbol{u}^h &= \begin{Bmatrix} u \\ v \\ w \end{Bmatrix} \\ &= \left[\phi_1\ \ \ldots\ \ \phi_n\right]\left[u_1, v_1, w_1, \ldots, u_n, v_n, w_n\right]^T \\ &= \boldsymbol{\Phi}_{3\times 3n}\boldsymbol{u}_{3n\times 1}\end{aligned} \tag{18}$$

where u, v, w are the components of displacement field of the deck and cables and $\Psi = \Psi(\mathrm{x})$ is the rotation of the deck about the x axis (longitudinal direction of the deck).

u_I, v_I and w_I are the parameters of displacements for *I*th node in the x ,y, z directions and θ_{xI}, θ_{yI} and θ_{zI} are parameters of rotations for *I*th node about the x ,y, z axis, respectively (see Fig. 2 for u_I, v_I and w_I as well as θ_{xI}, θ_{yI} andis the matrix of MLS shape $\mathbf{\Phi}$). θ_{zI} functions (Arzoumanidis and Bieniek 1985).

The strain components of deck consist of the axial strain, e_x, two curvatures, k_y and k_z, and the twist, t_x, writing as

$$\boldsymbol{\varepsilon}_{\boldsymbol{k}}^{\boldsymbol{T}} \equiv \left(e_x, k_y, k_z, t_x\right) \tag{19}$$

Whereas, the strain components of cable and hangers are only consisted of the axial strain, e_x .i.e., $\boldsymbol{\varepsilon}_{\boldsymbol{k}}^{\boldsymbol{T}} = e_x$ (Arzoumanidis and Bieniek 1985).

The strain-displacement relations are as follows:

$$\begin{gathered} \mathrm{e}_x = \frac{\partial u}{\partial x} + \frac{1}{2}\left(\frac{\partial u}{\partial x}\right)^2 + \frac{1}{2}\left(\frac{\partial v}{\partial x}\right)^2 + \frac{1}{2}\left(\frac{\partial w}{\partial x}\right)^2 \\ k_y = -\frac{\partial^2 v}{\partial x^2}, \quad k_z = -\frac{\partial^2 w}{\partial x^2}, \quad \mathrm{t}_x = \frac{\partial \Psi}{\partial x} \end{gathered} \tag{20}$$

From the definitions mentioned above and the relation (17), $\bar{\boldsymbol{B}}$ matrix of the node can be determined

$$\mathbf{d}\boldsymbol{\varepsilon}_{\boldsymbol{k}} = \bar{\boldsymbol{B}}\, \boldsymbol{du} \tag{21}$$

The matrix $\bar{\boldsymbol{B}}$ is decomposed in the following

$$\bar{\boldsymbol{B}} = \boldsymbol{B}_L + \boldsymbol{B}_{NL} \tag{22}$$

where $\boldsymbol{B}_L$ is a constant matrix corresponding to the linear terms in the strain displacement relations while $\boldsymbol{B}_{NL}$ represents the geometric nonlinearities (Arzoumanidis and Bieniek 1985).

The internal forces in the nodes of the deck bridge consisting of the normal force N_x, two bending moments M_y and M_z and the torsional moment T_x, i.e.

$$\boldsymbol{S_I}^{\boldsymbol{T}} = \left\{N_x, M_y, M_z, T_x\right\} \tag{23}$$

It should be noted that internal forces in the nodes of the cable and hangers system are only consist of the normal force, N_x. The computation of $\boldsymbol{S_I}$ in terms of $\boldsymbol{\varepsilon_k}$ is performed according to elastic theory of beams (Arzoumanidis and Bieniek 1985).

The final discrete equations can be achieved by substituting equations of approximate solution u and strains and internal forces into the weak form in Eq. (4), which yields

$$\mathbf{f}^{\mathbf{int}} + \mathbf{K}^{\alpha}\boldsymbol{U} = \mathbf{f}^{\mathbf{ext}} + \mathbf{F}^{\alpha} \tag{24}$$

where $\mathbf{K}^{\alpha}$ and $\boldsymbol{F}^{\alpha}$ are the global penalty stiffness and force matrices, respectively. Also, $\mathbf{U}$ presents the vector of nodal parameters of displacements for all nodes in the entire problem domain, $\mathbf{f}^{\mathbf{ext}}$ is the global external force vector assembled using the nodal force vectors $\boldsymbol{f}_I^{ext}$. The vector $\mathbf{f}^{\mathbf{int}}$ presents the global internal force vector. It is formed using the nodal internal force vectors $\boldsymbol{f}_I^{int}$. In Eq. (24), $\mathbf{K}^{\alpha}$, $\mathbf{f}^{\mathbf{int}}$, $\mathbf{f}^{\mathbf{ext}}$ and $\mathbf{F}^{\alpha}$ consist of sub-matrices $\boldsymbol{K}_{IJ}^{\alpha}$, $\boldsymbol{f}_I^{int}$, $\boldsymbol{f}_I^{ext}$ and $\boldsymbol{F}_I^{\alpha}$, given by

$$\boldsymbol{K}_{IJ}^{\alpha} = \int_{\Gamma_u} \boldsymbol{\Phi_I}^{\boldsymbol{T}} \boldsymbol{\alpha} \boldsymbol{\Phi_J}\, d\Gamma \tag{25}$$

$$\boldsymbol{f}_I^{int} = \int_x \bar{\boldsymbol{B}}_I^T \boldsymbol{\sigma_I}\, d\Omega \tag{26}$$

$$\boldsymbol{f}_I^{ext} = \int_{\Gamma} \boldsymbol{\Phi_I}^{\boldsymbol{T}} \bar{\boldsymbol{t}} d\Gamma + \int_{\Omega} \boldsymbol{\Phi_I}^{\boldsymbol{T}} \boldsymbol{b} d\Omega \tag{27}$$

$$\boldsymbol{F}_I^{\alpha} = \int_{\Gamma_u} \boldsymbol{\Phi_I}^{\boldsymbol{T}} \boldsymbol{\alpha} \bar{\boldsymbol{u}}\, d\Gamma \tag{28}$$

The tangent stiffness matrix of the *I*th node $\left(K_T\right)_I$ that plays a fundamental part in large deformation analysis, is defined by

$$\left(K_T\right)_I = \frac{\boldsymbol{d}\boldsymbol{f}_I^{int}}{\boldsymbol{du}} \tag{29}$$

In order to accomplish the numerical integrations in Eqs. (25) - (28), the problem domain is discretized into a set of background cells. The Gauss quadrature scheme is used to carry out the numerical integrations over these cells (Liu and Gu 2010). The nonlinear geometry is accounted by Updated Lagrangian description (Bathe 2006).

4. Aerostatic analysis of suspension bridges

In order to evaluate the aerostatic behaviors of suspension bridges, the following characteristics is considered: (1) the effect of three components of displacement-dependent wind loads and geometric nonlinearity of structure is simultaneously considered; (2) incremental-two-iterative solution scheme (Cheng, Jiang *et al*. 2002) is used to determine the wind velocity–deflection curve for a nonlinear aerostatic stability problem.

4.1 Wind loads

Generally the action of static wind loads on the bridge structure is recognized as the aerostatic effect. The aerostatic forces including the drag force, lift force and pitch moment (Fig. 3), vary as the bridge structure displaces, and is expressed as the function of the effective attack angle. As seen in Fig. 3, the effective angle of attack α is the sum of the wind angle of incidence and the torsional displacement of deck θ_x . The three components wind loads per unit length acting on the deformed deck (Fig. 3) which are dependent on torsional displacement of bridge structure, can be expressed as follows (Cheng, Jiang *et al.* 2002):

$$F_D = \frac{1}{2}\rho V_r^2 D C_D(\alpha) \tag{30a}$$

$$F_L = \frac{1}{2}\rho V_r^2 B C_L(\alpha) \tag{30b}$$

$$M_x = \frac{1}{2}\rho V_r^2 B^2 C_M(\alpha) \tag{30c}$$

where F_D , F_L and M_x are the aerodynamic drag, lift and moment, respectively, ρ is the air density, V_r is the mean velocity at the bridge deck level, D and B are the bridge deck height and width, respectively, $C_D(\alpha)$, $C_L(\alpha)$ and $C_M(\alpha)$ are the coefficients of drag force, lift force, and pitch moment in local bridge axes, respectively.

Generally, theoretical curves for the coefficients of the wind loads components ($C_D(\alpha)$, $C_L(\alpha)$ and $C_M(\alpha)$) which is derived by the experimental measurements are nonlinear. Curves for coefficients of drag force, lift force and pitch moment of wind loads are approximately estimated by linear segments between two experimental measurement points which can be written as

$$C_D(\alpha) = C_{Do} + \frac{\partial C_D}{\partial \alpha}\alpha \tag{31a}$$

$$C_L(\alpha) = C_{Lo} + \frac{\partial C_L}{\partial \alpha}\alpha \tag{31b}$$

$$C_M(\alpha) = C_{Mo} + \frac{\partial C_M}{\partial \alpha}\alpha \tag{31c}$$

where C_{Do} , C_{Lo} , C_{Mo} are wind load coefficients and $\frac{\partial C_D}{\partial \alpha}$, $\frac{\partial C_L}{\partial \alpha}$ and $\frac{\partial C_M}{\partial \alpha}$ are drag, lift and moment gradients (Arzoumanidis and Bieniek 1985).

4.2 Assumption

The first assumption is that the force-displacement transfer between the structure and the wind flow happens on the bridge deck and the cable systems (including suspended cable and hangers with no direct wind loading) only support the structural behavior of the deck. The second assumption is that vertical hangers connected to deck are distributed along the bridge length direction.

4.3 Solution algorithm

Since the displacement-dependent wind forces are considered as nonlinear functions of the wind attack angle, an incremental two-iterative solution scheme (Cheng Jiang *et al.* 2002) is used for solving nonlinear equation. Nonlinear analysis of bridge structure under any given wind velocity using Newton–Raphson method is performed in the inner loop of iteration. In the general loop of iterations, nonlinear analysis under the additional wind forces, induced by torsional deformations of the deck, is carried out. The computation procedure can be briefly expressed as follows:

(1) An initial wind velocity is considered. (2) The wind loads based on initial wind velocity are calculated. (3) The geometric nonlinear analysis of bridge structure under the aerostatic forces is performed by Newton–Raphson method and then the displacements are obtained. (4) Based on the obtained torsional angle of nodes, wind forces acting on the bridge structure under initial velocity is recalculate. (5) The state of convergence is determined whether the Euclidean norm of wind load coefficients is less than the prescribed tolerance. If the solution is convergent, increase wind velocity according to considered variation in wind velocity length. Otherwise, mentioned steps repeat until convergence is reach. (6) If the iterations do not converge for the given wind velocity, then get back previous wind velocity and calculate again by shortening length of wind velocity variation until the difference between two successive wind velocity is lower than the prescribed tolerance (Cheng *et al.* 2002). A flowchart for the solution procedure is given in Fig. 4.

5. Verification study

Based on the formulation and algorithm presented in previous sections, the numerical simulation is performed by programming in the MATLAB software framework for the nonlinear aerostatic stability analysis of suspension bridges. The accuracy of the programming is verified through following problems.

The first example is static problem which examine the ability of EFG method to model a cantilever beam under a transverse point load acting at the free end (Fig. 5). The utilized model takes into account the geometric nonlinearities and structural responses are determined through an iteration routine based on the Newton-Raphson method, in which the load was applied in a certain number of increments.

The schematic nodal distributions are shown in Fig. 5. The computational domain of the beam is exhibited by regularly distributed field nodes. In order to perform the numerical integrations, the regularly rectangular background cells are also employed. Three-point Gauss quadrature is used in each background cell. The circular support domains are chosen for the construction of meshfree shape functions and the size of support domains is also defined 2 times the nodal spacing. In order to impose essential boundary conditions, the penalty method is utilized (Liu and Gu 2010). In the EFG method, the

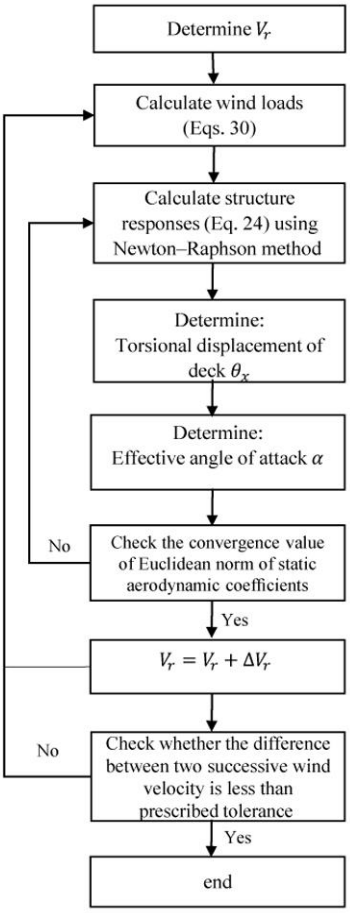

Fig. 4 Flowchart for solution procedure

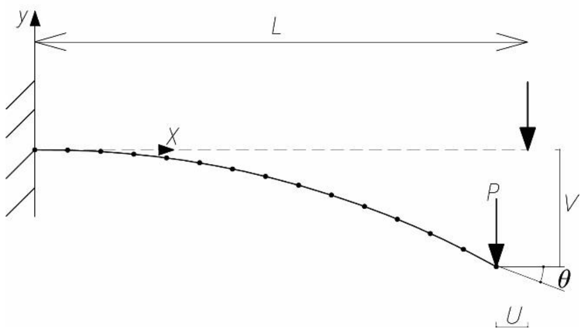

Fig. 5 Horizontal cantilever with a vertical point load at the free end

quadratic basis functions are used in the MLS approximation.

Investigation of above mentioned beam is also performed by the FEM. In FEM, nonlinear beam elements are utilized. The results acquired by the EFG method and FEM are compared to numerical results of Mattiasson (Mattiasson 1981) in Table 1. Comparisons of the displacement values obtained by both methods show good agreements with results of Mattiasson (Mattiasson 1981). However, the EFG method yields more accurate results compared with the FEM.

The second set of examples evaluates the results of nonlinear static analysis of the cable system of suspension bridge including suspended cable. The numerical simulation is performed by programming in the MATLAB software.

The material properties and geometric parameters of the cable system used in this study are presented in Table 2. For suspended cable, sag-to-span ratio is about one-tenth. The supports boundary conditions of cable system are considered as the hinged conditions. The domains used for the evaluation of the behavior of cables system are also indicated in Fig. 6.

The domain of the cable is presented by regularly distributed 201 field nodes and three -point Gauss quadrature is applied in all background cells. The linear basis functions are considered for the EFG interpolation. In the production of mesh free shape functions, the circular support domains are chosen and the dimension of support domains is also defined 2 times the nodal spacing. The penalty method is used for imposing the essential boundary conditions.

For numerical analysis, a suspended cable system subjected to point load is considered and the nonlinear geometry is included. The loads are applied in increments and the incremental load being applied to the equilibrium configuration of the previous load stage to obtain convergence condition. The initial position is considered as the self-weight equilibrium position.

The displacements under the specified load computed by EFG method are compared with the displacements obtained by modelling the cable using truss elements of FEM (Jayaraman and Knudson 1981) and are presented in Table 3. It can be observed that the results obtained by both numerical methods are coincident.

Presented test cases indicate that computed results by EFG method under large deformations demonstrate acceptable accuracy. From the CPU time consumption report in Table 1, it can be noticed that EFG method consumes more computational time in comparison to the classical FEM. However, since in EFG method for a problem domain does not require any mesh generation, total modeling efforts are less than methods like FEM. EFG method shows suitable accuracy in comparison to the classical FEM.

6. Case study

To investigate efficiency of the developed EFG method for modeling the nonlinear effects on the aerostatic behavior, the numerical analysis of a long-span suspension bridge under wind loads are evaluated. The wind loads are considered as a function of the torsional response of structure. The suspension bridge is analyzed using numerical procedure described in the preceding sections. The general configuration of the bridge is presented in Fig. 7. We investigate suspension bridge with a main span of 888 m and deck with 3.012 m depth and 35.6 m width; the spacing between the successive hangers is 12.0 m (Cheng Jiang *et al*. 2003). For suspended cable, sag-to-span ratio is considered about one-tenth. The mechanical properties of

Table 1 Deflections at the free end of the cantilever beam

	$\frac{u}{L}$			$\frac{v}{L}$			θ			CPU time (s)
$\frac{PL^2}{EI}$ Method	0.2	0.4	0.6	0.2	0.4	0.6	0.2	0.4	0.6	
EFG	0.00263	0.01037	0.00230	0.0662	0.1390	0.1937	0.09959	0.19732	0.2913	58.21
FEM	0.00273	0.01072	0.02397	0.06654	0.13233	0.196641	0.09972	0.19781	0.29268	27.3
Mattiasson (Mattiasson 1 981)	0.00265	0.01035	0.02249	0.06636	0.13098	0.19235	0.09964	0.19716	0.29074	-

the main members of bridge structure are presented in Table 4. It should be noted that elastic material properties is

Table 2 Numerical values of the cable system parameters

parameters	Suspended cable values
Length (m)	304.8
Young's modulus $\left(N/m^2\right)$	13357.7×10^7
Cross section area (cm^2)	5.4842
Weight $\left(N/m\right)$	47
Load point (KN)	35.586

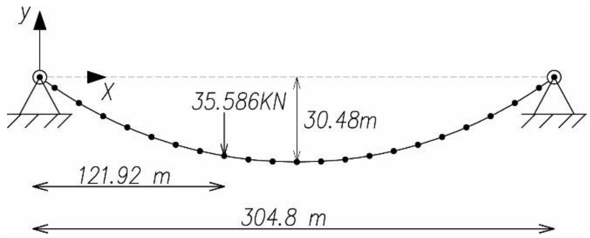

Fig. 6 Nodal arrangements used to model the cable system suspended cable

Table 3 Displacement under load

Displacement of load point (m)	EFG method	FEM using Truss element (Jayaraman and Knudson 1981)
Vertical	-5.4724	-5.472
Horizontal	-0.845	-0.845

considered in present analysis.

It should be stated that the utilized curves for coefficients of wind loads are those presented by Cheng *et al*. (2003). The coefficient curves of lift force and pitch moment of aerostatic loads are considered to be approximately linear, and linear curve fitting is employed. The static coefficients of wind loads for the studied bridge are given as follows (Cheng Jiang *et al*. 2003):

$$C_{Lo} = -0.02462, \quad \frac{\partial C_L}{\partial \alpha} = 0.0789 \tag{32a}$$

$$C_{Mo} = 0.00877, \quad \frac{\partial C_M}{\partial \alpha} = 0.01837 \tag{32b}$$

Furthermore, due to nonlinearity of the wind load coefficient curve of drag force, the nonlinear curve is piecewise linearized. The coefficients of drag force that are given by (Cheng, Jiang *et al*. 2003):

$$\begin{cases} C_{Do} = 0.81993 \quad , \dfrac{\partial C_D}{\partial \alpha} = 0.02075 & 0 \le \theta \le 1 \\ C_{Do} = 0.83759 \quad , \dfrac{\partial C_D}{\partial \alpha} = 0.00309 & 1 < \theta \le 2 \\ C_{Do} = 0.87531 \ , \dfrac{\partial C_D}{\partial \alpha} = -0.01577 & 2 < \theta \le 3 \\ C_{Do} = 0.9354 \ , \dfrac{\partial C_D}{\partial \alpha} = -0.0358 & 3 < \theta \le 4 \\ C_{Do} = 1.0202 \ , \dfrac{\partial C_D}{\partial \alpha} = -0.0577 & 4 < \theta \le \infty \end{cases} \tag{33}$$

An EFG model is developed for the evaluation of behavior of the considered suspension bridge. The numerical model takes the geometric nonlinearities into consideration. The computational domain shown in Fig. 7 is used for the study. The bridge deck segments are considered as continuous beam and the computational domain of the beam is considered by regularly distributed 149 field nodes. Also, for the evaluation of the behavior of suspended cables system is used regularly distributed 149 nodes in domain and the domains of hangers are also considered by regularly distributed nodes. In each rectangular background cell, three-point Gauss quadrature is used for performing numerical integration. The quadratic and linear basis functions (Liu and Gu 2010) are employed in the MLS approximation for the deck and cables, respectively. The circular support domains are considered for the determination of meshfree shape functions, and the size of support domains is also described 2 times the nodal spacing.

Lateral and vertical displacements of the bridge deck over the supports are restricted while the longitudinal displacement is only restricted at the left support. For the imposition of essential boundary conditions, the penalty method (Liu and Gu 2010) is used. The position of the hangers has been specified on the free cable. The three components of the displacement-dependent wind loads are only applied on the bridge deck and the effects of the aerostatic forces on the hangers and main cable are neglected.

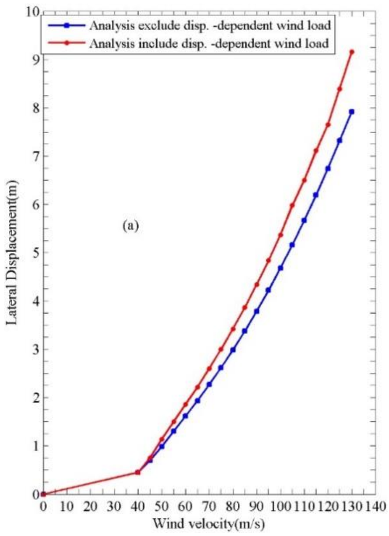

(a) Lateral displacement

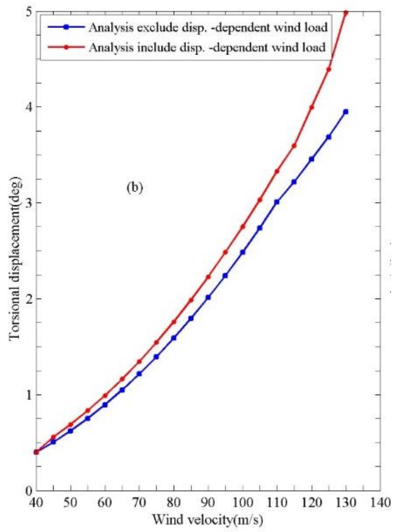

(b) Torsional displacement

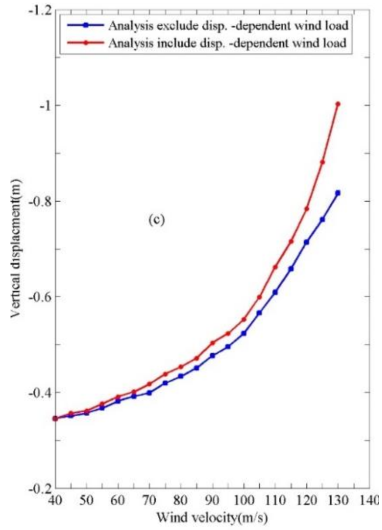

(c) Vertical displacement

Fig. 8 Responses at the center node of the main span, Comparison between aerostatic stability analysis including and excluding displacement-dependent wind loads (a) Lateral displacement (b) Torsional displacement (c) Vertical displacement

A, The cross sectional of area; E, modulus of elasticity; I_2, out-of-plane moments of inertia; I_3, in-

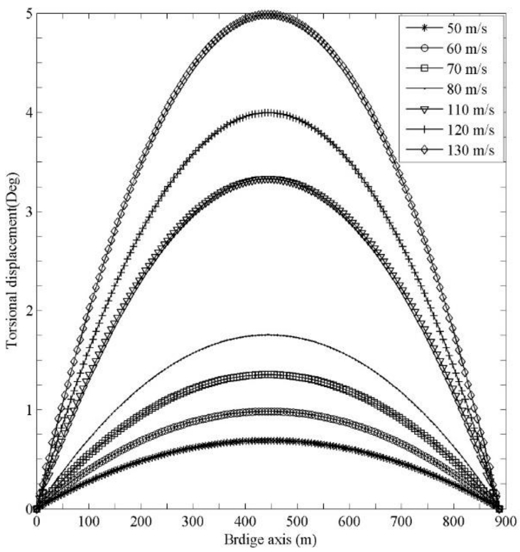

Fig. 9 Comparison of the torsional displacement of the deck at various wind velocities

Table 5 Comparison of critical wind speed in suspension bridge based on two methods

Type of analysis	Nonlinear aerostatic stability (Presented study)	Linear aerostatic stability (Xiang *et al*. 1996)	
		Lateral-torsional buckling	Torsional divergence
Critical wind speed $\left(m/s\right)$	130	165	136

plane moments of inertia; J : St. Venant constant; m, mass per unit length.

6.1 Aerostatic stability

In the present study, the linear and nonlinear aerostatic analysis are considered to investigate the torsional divergence of mentioned suspension bridge under displacement-dependent wind loads. In nonlinear analysis, the three components of displacement-dependent wind loads in addition to geometric nonlinearity are simultaneously considered. For comparison of computed results, the structural analysis has been also performed based on the linear theories in which the effect of torsional displacement of structure on the aerostatic forces is disregarded. It should be pointed out that aerostatic analysis under the initial wind attack angle equal to zero are carried.

Figs. 8(a), 8(b), and 8(c) indicate the lateral, torsional and vertical responses at the center node of the main span of bridge structure versus wind velocity. The presented results in Fig. 8 refer to the analysis based on including three components of displacement-dependent wind loads and excluding displacement-dependent wind load. It can be observed in the figures that the vertical, the lateral and the torsional responses for nonlinear analysis are larger than those for the condition of linear analysis at the same wind velocity. Hence, it can be stated that when the wind velocity reaches higher values, near to what might be the critical velocity of investigated suspension bridge, the differences between the responses of the linear and nonlinear analysis would appear. So it can be stated that the nonlinear effects caused by the deformation of the bridge deck influence the displacement responses of long-span suspension bridge and nonlinearity of the displacement responses of bridge under the displacement-dependent wind loads is observed.

Fig. 9 presents a comparison between the torsional responses of the bridge deck at several wind velocities along the bridge deck. It can be seen that torsional response of the deck increases significantly as wind speed increases. Also, results indicate that in wind speed 130 m/s in investigated bridge, increasing of torsional displacement is more obvious and it expects occurring torsional instability in studied bridge. The computed speed in this study is compared with linear aerostatic stability analysis of Xiang *et al*. (1996) based on simplified formula of torsional divergence and lateral-torsional buckling, as shown in Table 5. It can be also observed from Table 5 that the linear aerostatic stability analysis estimates more critical wind speed in contrast to nonlinear aerostatic stability analysis presented in this study. Generally, investigation of results obtained by the EFG method show that this method provides the suitable results in the aerostatic stability of suspension bridge.

7. Conclusions

An EFG structural solver is developed to predict aerostatic stability analysis of suspension bridge with a main span of 888 meters. The simultaneous influences of the geometric nonlinearity of structure and the three components of displacement-dependent wind loads on torsional divergence analysis of long-span suspension bridges are considered. Also, the numerical simulation has accounted for the elastic material properties.

The authors have implemented the EFG method in a program in the MATLAB software framework. Efficiency and accuracy of the implementation is verified through two examples of cantilever beam and suspended cable. The results of the EFG method indicate suitable accuracy in solution of large deformation structural problems. Although the EFG method does entail more computational costs for the analysis than methods based mesh, this shortcoming may be compensated by the ease of node generation task for the modeling of the problem domain in EFG method. The time consumption of EFG solver arises from the need to find the nodes within the domain of support of each Gauss point. However, since in EFG method for a problem domain does not require any mesh generation, total modeling efforts are less than based mesh methods like FEM. Meanwhile, EFG method obtains more accuracy results compared to the classical FEM.

Finally, in order to evaluate the performance of the EFG method, the numerical example of a long-span suspension bridge is investigated under wind loads to be the function of the torsional displacement of structure. The nonlinear effects induced by the static wind-structure interactions have affected the vertical, lateral and torsional displacements. Nonlinearity of the displacement responses of bridge structure under the displacement-dependent wind loads are observed. Therefore, in order to evaluate the aerostatic stability of long-span suspension bridges, nonlinear effects induced by the wind-structure interactions should be adopted.

Generally, the obtained results indicate that the EFG method is practical, and effective for modeling suspension bridge structure and also investigating the torsional divergence of suspension bridge. Finally, based on the numerical investigations of present work, we would highly recommend using the EFG method for analyzing the large deformation of structural cases under displacement-dependent wind loads which provides very promising method for analysis on stability of long-span suspension bridges under aerostatic forces.

However improving the techniques for finding the associated nodes of each support domain can speed up the computational procedure of the developed EFG solver for structures with large deformation.

Acknowledgments

The authors would like to express their personal thanks to Khajeh Nasir Toosi University for supporting this research work.

References

Arena, A., Lacarbonara, W. and Marzocca, P. (2016), "Post-critical behavior of suspension bridges under nonlinear aerodynamic loading", *J. Comput. Nonlinear Dyn*., **11**(1), 011005. https://doi.org/10.1115/1.4030040.

Arena, A., Lacarbonara, W., Valentine, D. and Marzocca, P. (2014), "Aeroelastic behavior of long-span suspension bridges under arbitrary wind profiles", *J. Flu. Struct*., **50**, 105-119.

https://doi.org/10.1016/j.jfluidstructs.2014.06.018.

Arzoumanidis, S.G. and Bieniek, M. (1985), "Finite element analysis of suspension bridges", Comput. Struct., **21**(6), 1237-1253. https://doi.org/10.1016/0045-7949(85)90178-6.

Bathe, K.J. (2006), "Finite element procedures", Klaus-Jurgen Bathe.

Boonyapinyo, V., Lauhatanon, Y. and Lukkunaprasit, P. (2006), "Nonlinear aerostatic stability analysis of suspension bridges", *Eng. Struct*., **28**(5), 793-803. https://doi.org/10.1016/j.engstruct.2005.10.008.

Cheng, J. (2000), "Study on nonlinear aerostatic stability of cable-supported bridges", Ph. D. Dissertation, Tongji University, Shanghai, China.

Cheng, J., Jiang, J.J. and Xiao, R.C. (2003), "Aerostatic stability analysis of suspension bridges under parametric uncertainty", *Eng. Struct*., **25**(13), 1675-1684. https://doi.org/10.1016/S0141-0296(03)00146-9.

Cheng, J., Jiang, J.J., Xiao, R.C. and Xiang, H.F. (2002), "Advanced aerostatic stability analysis of cable-stayed bridges using finite-element method", *Comput. Struct*., **80**(13), 1145-1158. https://doi.org/10.1016/S0045-7949(02)00079-2.

Cheng, J., Jiang, J.J., Xiao, R.C. and Xiang, H.F. (2002), "Nonlinear aerostatic stability analysis of Jiang Yin suspension bridge", *Eng. Struct*., **24**(6), 773-781. https://doi.org/10.1016/S0141-0296(02)00006-8.

Cheng, J., Xiao, R.C., Xiang, H.F. and Jiang, J.J. (2003), "NASAB: a finite element software for the nonlinear aerostatic stability analysis of cable-supported bridges", *Adv. Eng. Softw*., **34**(5), 287-296. https://doi.org/10.1016/S0965-9978(03)00010-3.

Diana, G., Fiammenghi, G., Belloli, M. and Rocchi, D. (2013), "Wind tunnel tests and numerical approach for long span bridges: the Messina bridge", *J. Wind Eng. Ind. Aerod*., **122**, 38-49.

Diana, G., Rocchi, D. and Belloli, M. (2015), "Wind tunnel: a fundamental tool for long-span bridge design", Struct. Infrastruct. Eng., 11(4), 533-555. https://doi.org/10.1016/j.jweia.2013.07.012.

Duan, Y., Xu, Y., Fei, Q., Wong, K., Chan, K., Ni, Y. and Ng, C. (2011), "Advanced finite element model of Tsing Ma Bridge for structural health monitoring", *Int. J. Struct. Stab. Dyn*., **11**(02), 313-344. https://doi.org/10.1142/S0219455411004117.

Ge, Y., Xia, J., Zhao, L. and Zhao, S. (2018), "Full aeroelastic model testing for examining wind-induced vibration of a 5,000 m spanned suspension bridge", *Front. Built Environ*., **4**, 20. https://doi.org/10.3389/fbuil.2018.00020.

Hirai, A., Okauchi, I., Ito, M. and Miyata, T. (1967), "Studies on the critical wind velocity for suspension bridges", *The Proceedings of the International Research Seminar on Wind Effects on Buildings and Structures*, University of Toronto Press Ontario, Canada, 81-103.

Hong, A.L., Ubertini, F. and Betti, R. (2011), "Wind analysis of a suspension bridge: identification and finite-element model simulation", *J. Struct. Eng*., **137**(1), 133-142. https://doi.org/10.1061/(ASCE)ST.1943-541X.0000279.

Jayaraman, H. and Knudson, W. (1981), "A curved element for the analysis of cable structures", *Comput. Struct*., **14**(3-4), 325-333. https://doi.org/10.1016/0045-7949(81)90016-X.

Kilic, S., Raatschen, H.J., Körfgen, B., Apaydin, N. and Astaneh-Asl, A. (2017), "FE model of the Fatih Sultan Mehmet Suspension Bridge using thin shell finite elements", *Arab. J. Sci. Eng*., **42**(3), 1103-1116.

Lancaster, P. and Salkauskas, K. (1981), "Surfaces generated by moving least squares methods", *Math. Comput*., **37**(155), 141-158. https://doi.org/10.1090/S0025-5718-1981-0616367-1.

Liu, G.R. and Gu, Y.T. (2010), "An Introduction to Meshfree Methods and Their Programming", Springer Publishing Company, Incorporated.

Mattiasson, K. (1981), "Numerical results from large deflection beam and frame problems analysed by means of elliptic integrals", *Int. J. Numer. Meth. Eng*., **17**(1), 145-153. https://doi.org/10.1002/nme.1620170113.

Petrini, F., Giuliano, F. and Bontempi, F. (2007), "Comparison of time domain techniques for the evaluation of the response and the stability in long span suspension bridges", *Comput. Struct*., **85**(11-14), 1032-1048. https://doi.org/10.1016/j.compstruc.2006.11.015.

Selvam, R.P., Govindaswamy, S. and Bosch, H. (2002), "Aeroelastic analysis of bridges using FEM and moving grids", *Wind Struct*., **5**(2_3_4), 257-266. https://doi.org/10.12989/was.2002.5.2_3_4.257.

Xiang, H., Lin, Z., Bao, W., Chen, A. and Gu, M. (1996), "Wind resistant design guidebook for highway bridges", People's Communication Press, Beijing.

Zhang, W.M., Ge, Y.J. and Levitan, M.L. (2013), "A method for nonlinear aerostatic stability analysis of long-span suspension bridges under yaw wind", *Wind Struct*., **17**(5), 553-564. https://doi.org/10.12989/was.2013.17.5.553.

Zhang, X., Xiang, H. and Sun, B. (2002), "Nonlinear aerostatic and aerodynamic analysis of long-span suspension bridges considering wind-structure interactions", *J. Wind Eng. Indus. Aerod*., **90**(9), 1065-1080. https://doi.org/10.1016/S0167-6105(02)00251-9.

Zhang, X.J. (2008), "Wind stability of three-tower suspension bridges", *Wind Struct*., **11**(4), 341-344. https://doi.org/10.12989/was.2008.11.4.341.

Zhang, X.J. (2011), "Investigation on the wind-induced instability of long-span suspension bridges with 3D cable system", *Wind Struct*., **14**(3), 209-220. https://doi.org/10.12989/was.2011.14.3.209.

FR